Journal of Alloys and Compounds 504S (2010) S460–S466

Contents lists available at ScienceDirect

Journal of Alloys and Compounds

journal homepage: www.elsevier.com/locate/jallcom

Microstructural evolution in friction stir welding of nanostructured ODS alloys

C.-L. Chen [a,*], G.J. Tatlock [b], A.R. Jones [b]

[a] Department of Materials Science and Engineering, I-Shou University, No. 1, Sec. 1, Syuecheng Road, Dashu Township, Kaohsiung 840, Taiwan
[b] Department of Engineering, The University of Liverpool, Liverpool, UK

ARTICLE INFO

Article history:
Received 27 June 2009
Received in revised form 22 January 2010
Accepted 28 February 2010
Available online 7 March 2010

Keywords:
Oxide dispersion strengthened alloys
Mechanical alloying
Friction stir welding
Electron backscatter diffraction

ABSTRACT

Nanostructured oxide dispersion strengthened (ODS) Fe-based alloys manufactured by mechanical alloying (MA) are generally considered to be promising candidate materials for high-temperature applications up to at least 1100 °C because of their excellent creep strength and good oxidation resistance. However, a key issue with these alloys is the difficulty in using fusion welding techniques to join components due to oxide particle agglomeration and loss in the weld zone and the disruption and discontinuity in the grain structure introduced at the bond. In this study, the evolution of microstructure has been comprehensively studied in friction stir welds in a ferritic ODS alloy. Initially, electron backscattering diffraction (EBSD) was used to analyze the grain orientation, the grain boundary geometries and recrystallization behaviour. It suggested that deformation heterogeneities were introduced during the friction stirring process which facilitated the onset of recrystallization. Transmission electron microscopy (TEM) and scanning transmission electron microscopy (STEM) were used to observe the effects of the friction stir welding (FSW) process on the grain structure and the distribution of Y_2O_3 and other particles in the metal substrates in the FSW and adjacent regions, after the alloys had been recrystallized at temperatures up to 1380 °C for 1 h in air. The results show that fine-equiaxed grains and a uniform distribution of oxide particles were present in the friction stirred region but that the grain boundaries in the parent metal were pinned by particles. Friction stirring appeared to release these boundaries and allowed secondary recrystallization to occur after further heat treatment. The FSW process appears to be a promising technique for joining ferritic ODS alloys in the form of sheet and tube.

1. Introduction

Iron-based oxide dispersion strengthened (ODS) alloys contain nanoscale and uniformly dispersed Y_2O_3 particles in a coarse elongated grain structure Fe–Cr–Al matrix. They exhibit excellent creep strength [1] and good oxidation resistance [2,3] and have potential for use in high-temperature applications such as boiler tubes, heat exchangers and combustion chambers [4–6]. In spite of their large stored energy content, ODS alloys produced by mechanical alloying, require heat treatment at temperatures close to their melting point, to develop their typical coarse grain structure. This unusual recrystallization behaviour is attributed to the presences of the nanoscale dispersion of oxide particles, which act as pinning points to inhibit dislocation movement in the metal matrix [7,8]. Additionally, with micron or sub-micron grain sizes in consolidated mechanically alloyed metals, the grain boundary junctions themselves may behave as pinning points for grain boundary bowing, suggesting a large activation energy for nucleation of recrystallization [9–11]. These unique properties affect recovery and recrystallization processes at high temperatures. Moreover, for creep applications, it is important to minimize the amount of the grain boundary area that is perpendicular to the principle loading direction [12]. Therefore, the as-produced, submicron fine-grained microstructure needs to be transformed into a coarse elongated grain structure with a high grain aspect ratio. This is achieved by secondary recrystallization through very high-temperature annealing (1380 °C, 1 h in laboratory air) in ODS alloys [13–16]. Additionally, annealing temperatures and oxide particles have a large effect on the microstructure development and these in turn affects the recrystallization behaviour [17].

However, a key issue with these alloys is the difficulty in retaining high-temperature strength across the joints in fabricated components, because traditional fusion welding processes lead to loss of the dispersoid. In particular, the nanoscale oxide particles float to the top of the molten weld pool to form an agglomeration resulting in loss of strength. The joining process also disrupts the beneficial high aspect ratio coarse grain structure and can lead to the undesirable formation of porosity. These changes lead to a significant decrease in high-temperature creep strength [18,19]. Friction stir welding (FSW) is a relatively new joining process invented by Thomas et al. [20,21] at the Welding Institute, Cambridge, UK in 1991, which is now commercially avail-

* Corresponding author. Tel.: +886 7 6577711x3118; fax: +886 7 6578444.
E-mail address: chunliang@isu.edu.tw (C.-L. Chen).

0925-8388/$ – see front matter © 2010 Elsevier B.V. All rights reserved.
doi:10.1016/j.jallcom.2010.02.192

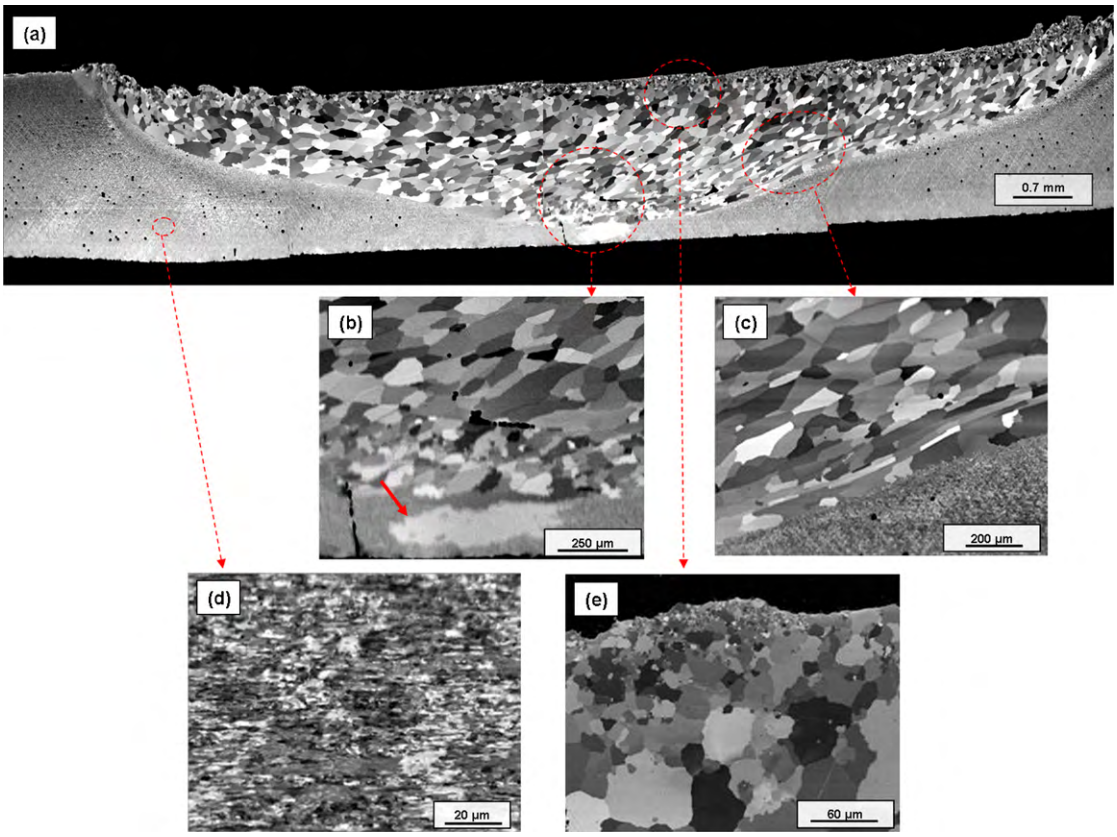

Fig. 1. Channeling contrast image showing: (a) the weld microstructure of PM2000 after the recrystallization treatment; (b) a large recrystallized grain on the bottom of the heat affect zone, (c)"onion-ring" structure; (d) a fine elongated grain structure showing in the non-FSW region and (e) small grains on the top of the FSW region.

able technology. FSW is a solid state welding/joining process which does not involve melting of the materials and has the potential to avoid significant microstructural or mechanical property changes in materials. FSW has been successfully applied to aluminium or even higher melting temperature materials (such as stainless steels, and Ni superalloys) which have exhibited excellent mechanical properties [22–24]. However, only a few authors have reported friction stir welding applications in ODS alloys [25–27]. Recrystallization behaviour of the friction stir weld remains unclear and has not been clarified yet.

Thus, the current study investigates the microstructures that form in friction stir welds in ODS alloy PM 2000 sheet following recrystallization treatment (1380 °C, 1 h in laboratory air). The microstructural changes, recrystallization behaviour and phase

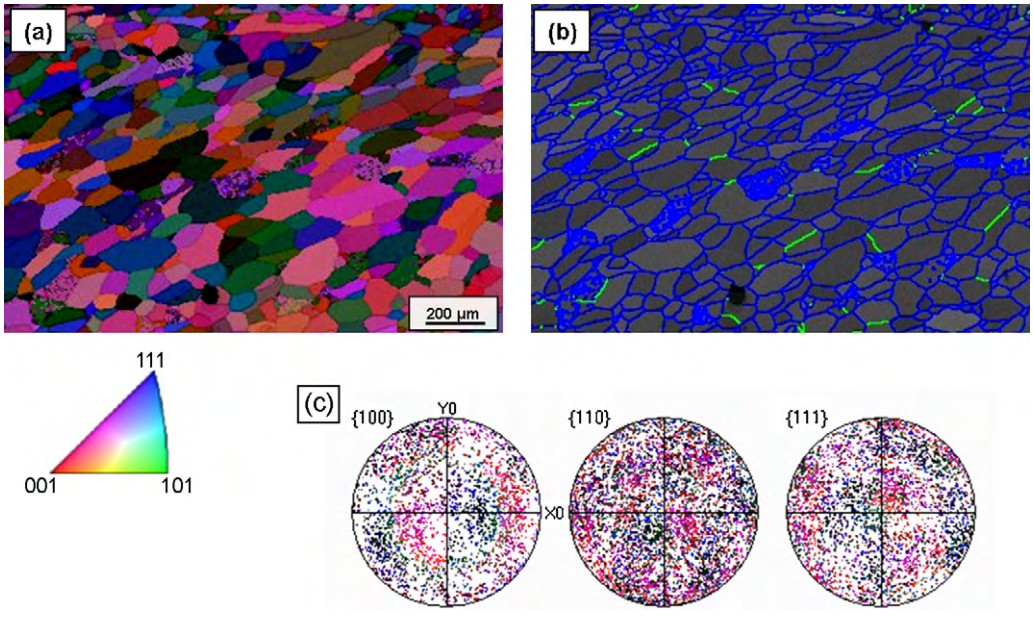

Fig. 2. EBSD mapping in the FSW region after the recrystallization treatment: (a) grain orientation map, (b) grain boundary misorientation angle map and (c) pole figures.

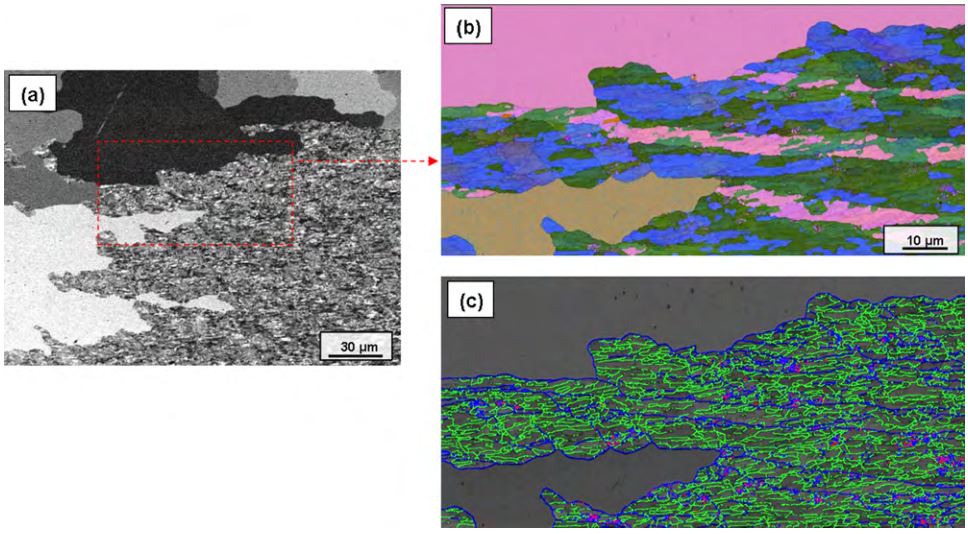

Fig. 3. The microstructure of the HAZ boundary zone after the recrystallization treatment: (a) an SEM channelling contrast image, (b) grain orientation map and (c) grain boundary misorientation angle map.

Table 1
Chemical composition of PM2000 (wt.%).

Fe	Cr	Al	Ti	Y_2O_3
Balance	20	5.5	0.5	0.5

transformation were analyzed using advanced electron microscopy techniques.

2. Experimental procedure

The alloy studied was a PM2000 sheet, oxide dispersion strengthened alloy produced by Plansee GmbH. The nominal chemical composition is given in Table 1. The high aluminium and chromium levels impart good oxidation and corrosion resistance. It was produced by mechanical alloying using a high-energy ball mill and various precursor powders (in the size range 1–200 μm) e.g. master alloy, Y-oxide etc. Consolidation of powders involves extrusion or hot compaction, following which the alloy is hot or cold rolled. The alloy was supplied as 2 mm thick sheet in a fine-grained condition.

In the friction stir welding process a cylindrical and shouldered tool with an extended pin (probe) is rotated and gradually plunged into the joint between the metals to be joined. Bonding is achieved by the combination of frictional heat and forging which is generated when the probe enters the workpiece creating a plasticised region in the workpiece material around the probe. No extra filler material was used.

In this study, the microstructure of the ODS alloys was examined in the FSW and adjacent regions, both after welding and after the alloys had been annealed at temperatures up to 1380 °C for 1 h in air. A CamScan X500 Field Emission Gun Scanning Electron Microscope (FEG-SEM) equipped with electron backscattering diffraction (EBSD) was used to analyze the grain orientation, the grain boundary geometries and recrystallization behaviour. All crystallographic orientation data were collected by electron backscatter patterns and processed using the software package CHANNEL 5. Transmission electron microscopy (TEM) was performed on a JEOL 2000FX instrument operating at 200 kV to exam the grain structure and dislocations. The size distribution of the Y–Al–O particles was investigated by scanning transmission electron microscopy (VG Microscopes HB601 field emission gun STEM operating at 100 kV). Samples of oxide particles were prepared for analysis using carbon extraction replicas to eliminate ferromagnetic effects from the matrix to increase resolution and enable simpler determination of particle chemical compo-

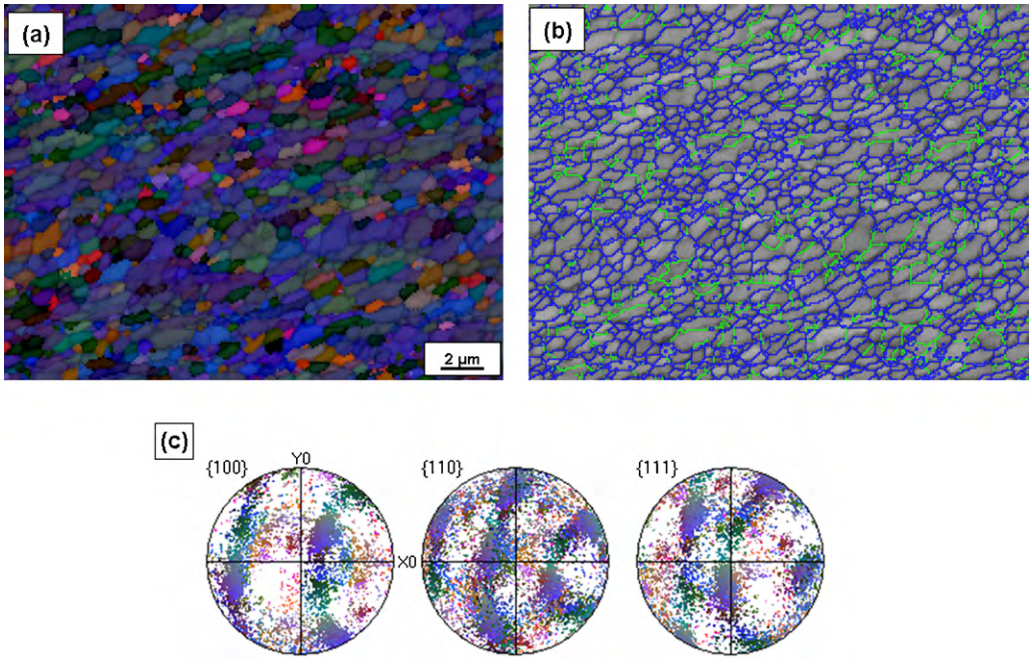

Fig. 4. EBSD mapping in the FSW region before the recrystallization treatment: (a) grain orientation map, (b) grain boundary misorientation angle map and (c) pole figures.

sition. Chemical etching for extraction of the oxide particles was performed using a 10% HCl methanol solution.

3. Results and discussion

3.1. SEM examinations

A typical channelling contrast image, Fig. 1a, shows a large grained, recrystallized, equiaxed structure in the weld region following recrystallization annealing. On the right hand side of the weld region, Fig. 1c, it appears that cylindrical sheets of material have been extended during each rotation of the threaded tool, depositing material from the front to the back of the weld. This manifests itself as a characteristic 'onion-ring' structure.

A large recrystallized grain was also found at the bottom of the heat affected zone (HAZ) in parent sheet near the boundary region, as shown in Fig. 1b. It is believed that a large strain was generated in this region during the FSW processing where deformation heterogeneities facilitated the onset of recrystallization. This also suggests that any inhomogeneity of stored energy would affect the nucleation of recrystallization. However, in the non-FSW region, Fig. 1d, it shows a fine-scale, elongated grain structure. This implies that only recovery had taken place. The details will be discussed later where EBSD and TEM data are presented. Additionally, small voids were observed throughout the non-FSW region, possibly due to diffusion of gas entrapped during the powder milling process. It was observed that much finer recrystallized grains were formed along the top of the weld region, as shown in Fig. 1e. This may have been an effect due to the cooling rate or may be a local effect attributable to the shoulder of the FSW tool local to the sample surface, introducing local deformation heterogeneity which provides numerous nucleation sits for recrystallization.

3.2. EBSD analysis

EBSD was used to investigate grain orientation and the grain boundary geometries. Fig. 2a shows the orientation map in the exact central region of the FSW zone following recrystallization annealing, exhibiting distinct grains and sub-structures and varied grain orientations highlighted with different colours. Each crystal orientation point corresponds to a fixed direction in the sample and the colour to use in the map is found on the colour key. The pole figures, Fig. 2c, suggest that grains were oriented much more randomly with fewer preferred orientations compared to the parent metal. The grain boundary misorientation angle map reveals important details of the sub-structure, as shown in Fig. 2b. The high energy, high-angle boundaries are decorated with blue lines

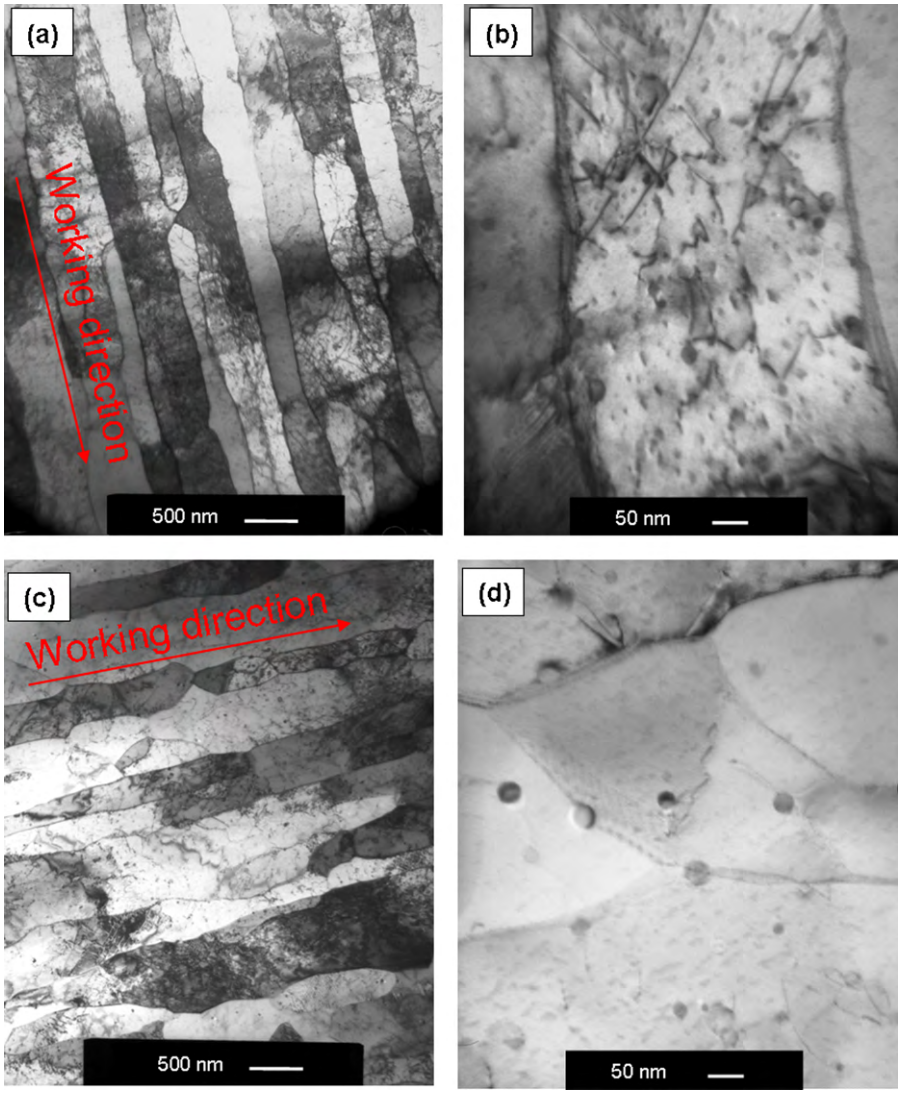

Fig. 5. TEM micrographs of the non-FSW region (a) and (b) before and (c) and (d) after the recrystallization treatment.

(for misorientations >10) and can be seen to comprise the majority of the boundaries after recrystallization. A more detailed analysis shows that the high-angle boundaries are most commonly found with an angular misorientation in the range 40–55°.

An interesting region at the edge of the HAZ, shown in Fig. 3a, was investigated. The grain orientation of this region is shown in Fig. 3b. The large recrystallized grains display high angle boundaries while the elongated grains, which consist of numerous subgrains with an irregular morphology, exhibit many low angle boundaries (green lines; less then 10° misorientation), as seen in Fig. 3c. On the basis of these data, it is reasonable to assume that in the non-FSW region only recovery has taken place, recrystallization possibly having been hindered by strong local association between dispersoid particles and the low angle grain boundary structures present in the parent sheet. In this case, large recrystallized grains have grown out from the join region into the adjacent recovered subgrain structures.

The EBSD orientation map of the FSW region before the recrystallization treatment is shown in Fig. 4a. It is characterised by a fine (~1 μm) equiaxed grain structure mainly separated by high angle grain boundaries highlighted in blue, in Fig. 4b. This suggests that the elongated grains can be dynamically recrystallized to a sub-micron primary recrystallised grain size during the FSW process. The stirring action of the rotating welding tool generates a shear deformation texture, which corresponds to rotation of grains in the surrounding materials, as shown in the pole Fig. 4c. The blue and purple orientations predominate in the FSW region where the grains rotate in response to the preferred orientation.

3.3. TEM observations

TEM observations provided details of the grain structures, deformation behaviour and dislocation interactions in the various conditions (FSW and non-FSW regions, before and after the recrystallization treatment). Fig. 5a shows the microstructure of the non-FSW region before the recrystallization treatment. The fine-grains were elongated and aligned with the working direction and contained a large number of particles. The region was characterised by high dislocation density accumulated within low angle boundary structures, clearly visible in the TEM micrographs. Additionally, the fine oxide particles tended to be aligned along the grain boundaries. Closer inspection, as in Fig. 5b, revealed evidence of particle–subgrain boundary interactions in the microstructure

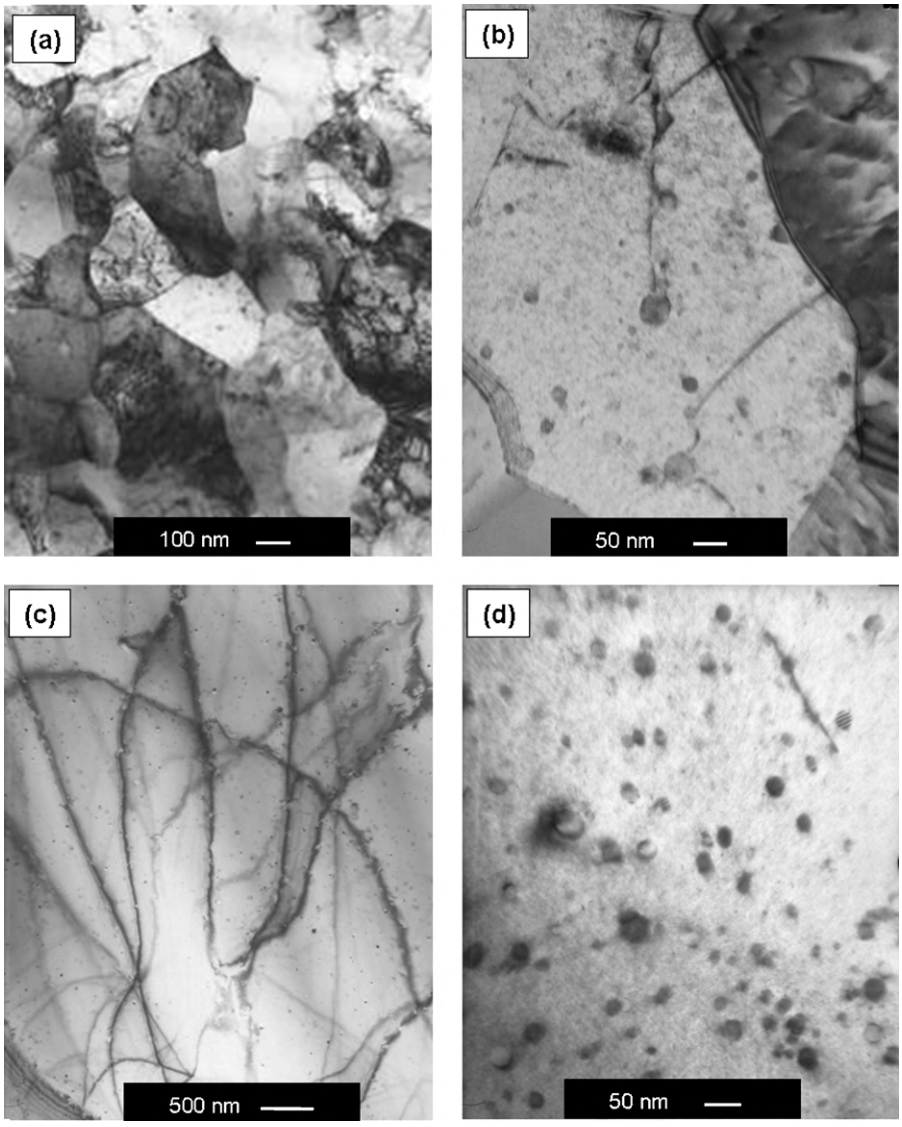

Fig. 6. TEM micrographs of the FSW region (a) and (b) before and (c) and (d) after the recrystallization treatment.

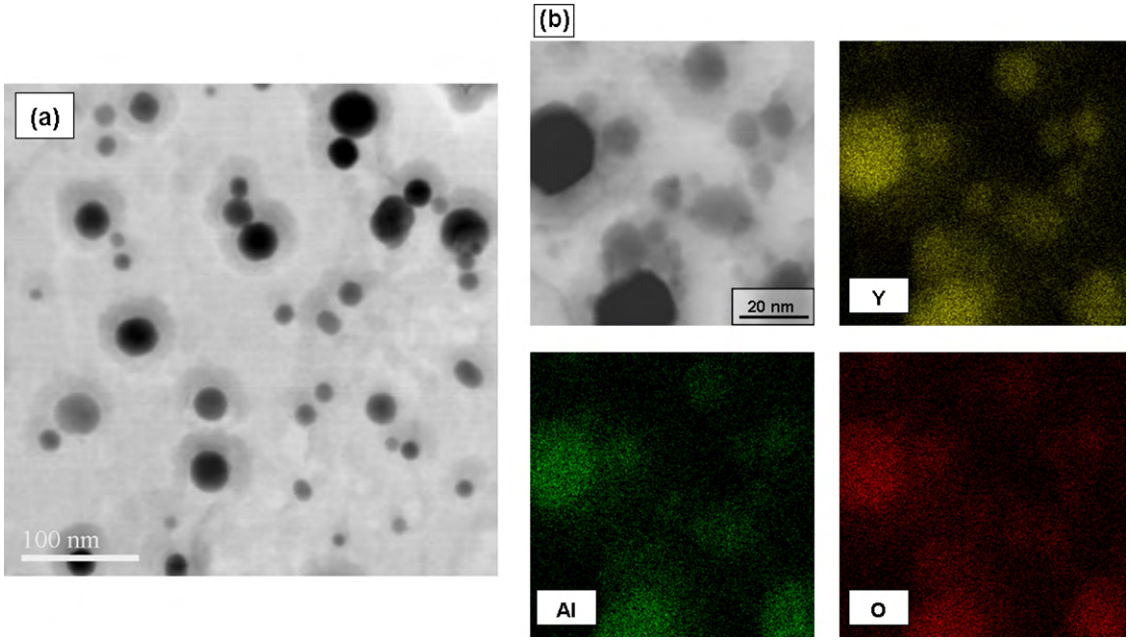

Fig. 7. (a) BF-STEM image shows distribution of nanoscale Y–Al–O particles and (b) EDS mapping of an area of interest from an extraction replica sample.

typical of Zener pinning, inhibiting dislocation rearrangement subsequent recovery and recrystallization processes.

Fig. 5c shows the microstructure of the non-FSW region after the recrystallization treatment. The elongated grains and particles coarsen slightly after the treatment and consist of distinct subgrains with low angle boundaries. The dislocation density inside these subgrains was reduced as a result of recovery. The particles have tended to pin and stabilize the dislocation substructures, as shown in Fig. 5d. Note that the subgrain boundaries may still be able to migrate at this stage.

On the other hand, Fig. 6a shows the microstructure of the FSW region before the recrystallization treatment. A fine-equiaxed grain structure with low dislocation density was shown to be present. The result corresponds to the EBSD analysis, which suggests that the elongated grains in parent sheet can be dynamically recrystallized to a sub-micron grain size during the FSW process. The particles were distributed randomly in the matrix and Zener pinning and subgrains were still visible at this stage, as shown in Fig. 6b. However, no significant evidence was observed for continuing alignment of fine oxide particles along grain boundaries. This can be attributed to the homogenisation effects of the FSW process.

Fig. 6c shows the microstructure of the FSW region after the recrystallization treatment. Large areas were dislocation free and few grain boundaries were observed in the microstructure. It confirms that subsequent heat treatment leads to secondary recrstallization driven by the grain boundary energy of the fine-grained primary recrystallised state. In addition, the distribution of the particles is uniform although they may be slightly coarser after the annealing treatment, as shown in Fig. 6d.

3.4. STEM investigations

STEM was used to measure particle sizes and distributions on samples prepared as extraction replicas. Fig. 7a shows a BF-STEM micrograph of the oxide particle distribution in the FSW region after recrystallization treatment. Oxide dispersoid particles were homogenously distributed in the sample and their diameters varied from 5 to 70 nm. The particles all had a spherical morphology and were identified as Y–Al–O compounds by EDS analyses in STEM, as shown in Table 2 and the EDS maps shown in Fig. 7b. Note that coarse particles such as α-Al_2O_3 or Ti(C,N) inclusions are unlikely to be seen in the microstructure due to the difficulty of extracting large particles using this technique. The size distribution of Y–Al–O particles obtained from 121 particles from six BF-STEM micrographs. The mean particle diameter was 21 nm and most of the particles are between 10 and 30 nm. The result is in a good agreement with large scale measurements using neutron scattering [28].

Table 2
A typical composition of Y–Al–O particle.

at%	O	Al	Y
Y–Al–O	44.2	28.3	27.4

4. Conclusions

Friction stir welding appears to be a very promising technique for the joining of ODS materials in the form of sheet and tube. EBSD analysis confirms that low angle grain boundary migration occurs during recovery and high angle grain boundary migration occurs during recrystallization. Alloy microstructures in friction stirred samples, observed by TEM, suggested that the oxide particles were uniformly distributed by friction stirring but that the grain boundaries in the parent metal were pinned by particles. Friction stirring appeared to release these boundaries and allowed secondary recrystallization to occur after further heat treatment. STEM investigation suggests that the mean size of Y–Al oxide particle is 21 nm, which is a good agreement with large scale measurements using neutron scattering.

Acknowledgements

The financial support of the UK Department for Business and Enterprise and Regulatory Reform (BERR) as part of a US/UK collaboration on Advanced Materials is gratefully acknowledged. We are also pleased to acknowledge useful discussions with members of Prof. David Prior's EBSD group.

References

[1] J.D. Whittenberger, Metall. Trans. A 12 (1981) 845–851.
[2] T.A. Ramanarayanan, R. Ayer, R. Petkovic-Luton, D.P. Leta, Oxid. Met. 29 (1988) 445–472.
[3] W.J. Quadakkers, K. Bongartz, Mater. Corros. 45 (1994) 232–241.
[4] I. Baker, Mater. Sci. Eng. A 193 (1995) 1–13.
[5] I. Baker, P.R. Munroe, Int. Mater. Rev. 42 (1997) 181–205.
[6] N.S. Stoloff, Mater. Sci. Eng. A 258 (1998) 1–14.
[7] K. Murakami, K. Mino, H. Harada, H.K.D.H. Bhadeshia, Metall. Trans. A 25 (1994) 652–653.
[8] F. Starr, A.R. White, B. Kazimierza, Proceedings of Materials Advanced Power Engineering, Kluwer Academic Pub., Liege, 1994, p. 1393.
[9] C. Capdevila, H.K.D.H. Bhadeshia, Adv. Eng. Mater. 3 (2001) 647–656.
[10] H.K.D.H. Bhadeshia, Mater. Sci. Eng. A 223 (1997) 64–77.
[11] K. Mino, H. Harada, H.K.D.H. Bhadeshia, M. Yamazaki, Mater. Sci. Forum. 88–90 (1992) 213–220.
[12] D.M. Jaeger, The development of microstructure and its influence on stress rupture failure in iron based ods alloys by mechanical alloying, PhD Thesis, The University of Liverpool, 1994.
[13] T.S. Chou, H.K.D.H. Bhadeshia, Mater. Sci. Technol. 9 (1993) 890–897.
[14] W. Sha, H.K.D.H. Bhadeshia, Metall. Trans. 25A (1994) 705–714.
[15] W. Sha, H.K.D.H. Bhadeshia, J. Mater. Sci. 30 (1995) 1439–1444.
[16] M. Mujahid, J.W. Martin, Mater. Sci. Technol. 10 (1994) 703–710.
[17] C.-L. Chen, G.J. Tatlock, A.R. Jones, J. Microsc. 233 (2009) 474–481.
[18] H.D. Hedrich, H.D. Mayer, G. Haufler, M. Kopf, N. Reheis, Proceedings of the Conference on Materials for Advanced Power Engineering, Kluwer Academic Publishers, Dordrecht, 1994, pp. 789–798.
[19] M.A. Harper, Development of ODS Heat Exchanger Tubing, Special Metals Corporation, Huntington, KY, 2003.
[20] W.M. Thomas, E.D. Nicholas, J.C. Needham, M.G. Murch, P. Temple-Smith, C.J. Dawes, Friction stir butt welding, Int. Patent Application no. PCT/GB92/02203; GB Patent Application no. 9,125,978.8 (1991); US Patent no. 5,460,317 (1995).
[21] W.M. Thomas, E.D. Nicholas, J.C. Needham, M.G. Murch, P. Temple-Smith, C.J. Dawes, Improvements relating to friction welding, International Patent Classifications B23K 20/12, B29C 65/06, 1993.
[22] J.Q. Su, T.W. Nelson, R. Mishra, et al., Acta Mater. 3 (2003) 713–729.
[23] R.S. Mishra, Z.Y. Ma, Mater. Sci. Eng. R 50 (2005) 1–78.
[24] Y.S. Sato, P. Arkom, H. Kokawa, et al., Mater. Sci. Eng. A 477 (2008) 250–258.
[25] M.H. Mathon, V. Klosek, Y. de Carlan, et al., J. Nucl. Mater. 386 (2009) 475–478.
[26] F. Legendre, S. Poissonnet, P. Bonnaillie, et al., J. Nucl. Mater. 386 (2009) 537–539.
[27] C.L. Chen, P. Wang, G.J. Tatlock, Mater. High Temp. 26 (2009) 299–303.
[28] G. Muralidharan, preliminary measurement of oxide particle size distribution using neutron scattering by staff at Oak Ridge National Laboratory (ORNL) (private communication).